

# Non-Fermi-liquid behavior and anomalous suppression of Landau damping in layered metals close to ferromagnetism

Sam P. Ridgway and Chris A. Hooley

*Scottish Universities Physics Alliance, School of Physics and Astronomy,  
University of St Andrews, North Haugh, St Andrews, Fife KY16 9SS, United Kingdom*

(Dated: November 1, 2018)

We analyse the low-energy physics of nearly ferromagnetic metals in two spatial dimensions using the functional renormalization group technique. We find a new class of low-energy fixed point, at which the fermionic (electron-like) excitations are non-Fermi-liquid ( $z_f = 7/6$ ) and the magnetic fluctuations exhibit an anomalous Landau damping whose rate vanishes as  $\Gamma_{\mathbf{q}} \sim |\mathbf{q}|^{1/3}$  in the low- $|\mathbf{q}|$  limit. We discuss the physical nature of this fixed point, and highlight its possible applicability to experiments on  $\text{UGe}_2$  and related compounds.

PACS numbers: 71.27.+a, 71.10.Hf, 64.70.Tg

*Introduction.* The problem of describing the low-temperature behavior of metals close to a magnetic instability is now several decades old, and many experimental examples are available. These include the cuprate superconductors [1], heavy fermion materials [2, 3], and nearly ferromagnetic metals [4]. Among the phenomena observed in them are non-Fermi-liquid behavior of the conduction electrons, anomalous power laws in thermodynamic observables, and the emergence of new phases in the vicinity of the instability point. That point is commonly modelled by coupling fermions with a gapless Fermi surface (the electrons) to a massless boson (representing the magnetic fluctuations).

The distinction between an instability to ferromagnetism and an instability to antiferromagnetism is an important one, both experimentally and theoretically. For incipient antiferromagnets, the magnetic fluctuations are peaked at some non-zero wavevector  $\mathbf{Q}$ , and typically scatter the electrons between certain ‘hot spots’ on the Fermi surface. This leads naturally to theories in which the Fermi surface is divided into patches. In the ferromagnetic case, however, the magnetic fluctuations are peaked at  $\mathbf{Q} = \mathbf{0}$ , which implies strong forward scattering at every point on the Fermi surface. In this Letter we address the ferromagnetic version of the problem. This is a strong-coupling problem in two spatial dimensions, which is the case we shall concentrate on here.

A key obstacle to theoretical progress is that, due to the quantum-mechanical effects that prevail at such low temperatures, one cannot separate the static and dynamic properties of the system. To address this issue, Hertz put forward his theory of quantum criticality in the 1970s [5]. An important physical ingredient of the Hertz theory is Landau damping: the decay of magnetic fluctuations into quasiparticle-quasihole pairs. Hertz integrated out the fermions to produce a purely bosonic description of the quantum critical point [5, 6]: the boson propagator is modified by the Landau damping term in the expansion of the particle-hole bubble, enforcing a bosonic dynamical exponent  $z_b = 3$ , and the critical point is reduced

to a conventional scalar field theory. But the Hertz theory is unsatisfactory, as it assumes a Fermi-liquid form of the fermion propagator. In addition, more careful analyses suggest that multi-paramagnon interactions become singular, rendering a purely bosonic description invalid [5, 7].

The failure of Hertz-type theories has motivated a concentration on theories that retain both the electronic (fermionic) and magnetic (bosonic) degrees of freedom in their low-energy description. Such a theory may be treated by the standard Wilsonian renormalization approach [8, 9]; this results in a non-Fermi liquid fixed point in an expansion in  $\epsilon = 3 - d$ . However, this approach does not capture the onset of Landau damping, and thus gives physically incorrect results at low energies.

An alternative approach is the diagrammatic one, which proceeds by calculating the one-loop fermionic self energy using the Landau-damped propagator of Hertz theory. The one-loop dynamic self-energy scales as  $\omega^{2/3}$  [10–13], dominating the bare dynamic term  $\omega$  in the low-energy limit. Despite the fact that the procedure used to obtain this result is clearly not self-consistent, the  $\omega^{2/3}$  form of the self-energy was argued to be exact by Rech *et al.* [14], via an Eliashberg approach which is controlled by a large- $N_f$  limit. However, Sung-Sik Lee [15] showed that a class of planar diagrams causes the large- $N_f$  methods to fail below a certain energy scale; this was confirmed by explicit three-loop calculations by Metlitski and Sachdev [16]. Thus, despite recent intensive work [17–20], the problem of fermions interacting with an overdamped bosonic mode remains unsolved.

In this work, we present a functional renormalization group (fRG) analysis of the ferromagnetic critical point, explicitly including Landau damping, using a method recently applied by Lee, Strack, and Sachdev to an antiferromagnetic quantum critical point in a lattice model [21]. Our approach relies neither on a patch method nor on a large- $N_f$  expansion [22]. As we shall show, fRG analysis of this model yields a new type of low-energy fixed point in which a non-Fermi-liquid electronic sector

interacts with a peculiar type of overdamped magnetic excitation.

*Flow equations.* We begin with a model of fermions  $\psi$  with a circular Fermi surface, and couple these to a bosonic field  $\phi$  via a Yukawa coupling  $g$ , giving the microscopic action

$$S = - \int_{\omega \mathbf{k}} \bar{\psi}_{\omega \mathbf{k}} (i\omega - \tilde{k}) \psi_{\omega \mathbf{k}} + \int_{\Omega \mathbf{q}} \phi_{\Omega \mathbf{q}}^* (|\mathbf{q}|^2 + m^2) \phi_{\Omega \mathbf{q}} + g \int_{\omega \mathbf{k}} \int_{\Omega \mathbf{q}} \bar{\psi}_{\omega+\Omega, \mathbf{k}+\mathbf{q}} \psi_{\omega \mathbf{k}} \phi_{\Omega \mathbf{q}}. \quad (1)$$

Here  $\tilde{k} \equiv |\mathbf{k}| - k_F$  describes the linearized dispersion of the fermions near the Fermi momentum  $k_F$ , and  $m$  is the boson mass, which is set to zero since we work at criticality. We use the notation  $\int_{\omega \mathbf{k}} = (2\pi)^{-3} \int_{-\infty}^{\infty} d\omega \int^{|\tilde{k}| < \Lambda_{UV}} d^2 \mathbf{k}$  and  $\int_{\Omega \mathbf{q}} = (2\pi)^{-3} \int_{-\infty}^{\infty} d\Omega \int^{|\mathbf{q}| < \Lambda_{UV}} d^2 \mathbf{q}$ , where  $\Lambda_{UV} \ll k_F$  is an ultraviolet cutoff. Note that we do not include any dynamics of the boson in the bare action (1); the dynamics will be generated via the interactions with the fermions.

Following the usual fRG procedure, we follow the flow of the generating functional of one-particle irreducible vertex functions  $\Gamma_R^\Lambda$  as the infrared scale  $\Lambda$  is reduced from  $\Lambda_{UV}$  to zero [23–25]:

$$\frac{d}{d\Lambda} \Gamma_R^\Lambda = \frac{1}{2} \text{STr} \left( \partial_\Lambda R^\Lambda \left[ \Gamma_R^{(2)\Lambda} + R^\Lambda \right]^{-1} \right). \quad (2)$$

The generating functional  $\Gamma_R^\Lambda$  flows from the microscopic action  $\Gamma_R^{\Lambda_{UV}} = S$  to the effective action  $\Gamma_R^{\Lambda \rightarrow 0} = \Gamma$ . Our truncation of  $\Gamma_R^\Lambda$  includes only the dressed fermionic propagator  $G_f^\Lambda$ , the dressed bosonic propagator  $D_b^\Lambda$ , and the Yukawa coupling  $g^\Lambda$ . The regulator  $R^\Lambda$  cuts off the infrared divergences in the fermionic and bosonic propagators; however, in order to capture the physics of Landau damping — which is generated only by low-energy fermions — we must follow Lee, Strack, and Sachdev [21] and set the fermionic regulator function to zero.

The fermionic matrix element of  $\Gamma_R^{(2)\Lambda} + R^\Lambda$  is given by

$$G_f^\Lambda(\omega, \mathbf{k}) = \left( i\omega - \tilde{k} - \Sigma_f^\Lambda(\omega, \mathbf{k}) \right)^{-1}, \quad (3)$$

where  $\Sigma_f^\Lambda(\omega, \mathbf{k})$  represents the fermion self energy. We will only be interested in the low energy behavior of the model and so will parameterize the self energy as

$$\Sigma_f^\Lambda(\omega, \mathbf{k}) = (1 - A_\omega^\Lambda) i\omega - (1 - A_k^\Lambda) \tilde{k}, \quad (4)$$

where the Fermi momentum has been kept fixed. We may use these parameters to calculate the renormalized Fermi velocity,  $v_f^\Lambda = A_k^\Lambda / A_\omega^\Lambda$ , and the quasiparticle weight,  $Z_f^\Lambda = 1 / A_\omega^\Lambda$ , at all stages of the flow.

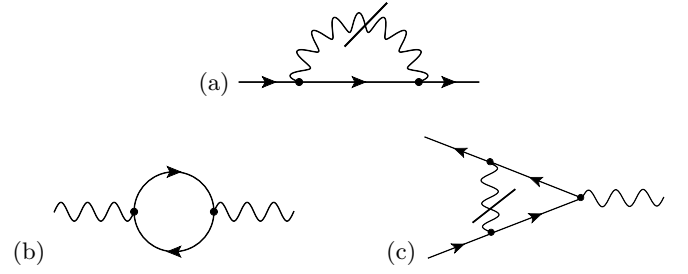


FIG. 1. The diagrams governing the fRG flow of (a) the fermionic self-energy  $\Sigma_f^\Lambda$ , (b) the bosonic self-energy  $\Sigma_b^\Lambda$ , and (c) the Yukawa coupling,  $g^\Lambda$ . The dash indicates a derivative with respect to the bosonic regulator.

The flow of the fermion self energy, corresponding to the diagram shown in Fig. 1(a), is given by

$$\partial_\Lambda \Sigma_f^\Lambda(\mathbf{k}, \omega) = (g^\Lambda)^2 \int_{\Omega \mathbf{q}}^R G_f^\Lambda(\omega + \Omega, \mathbf{k} + \mathbf{q}) D_b^\Lambda(\Omega, \mathbf{q}), \quad (5)$$

where  $\int_{\Omega \mathbf{q}}^R = \int_{\Omega \mathbf{q}} (-\partial_\Lambda R^\Lambda) \partial_{R^\Lambda}$  acts on the bosonic propagator.

The bosonic matrix element of  $\Gamma_R^{(2)\Lambda} + R^\Lambda$  is given by

$$D_b^\Lambda(\Omega, \mathbf{q}) = - \left( \max(|\mathbf{q}|^2, \Lambda^2) + \Sigma_b^\Lambda(\Omega, \mathbf{q}) \right)^{-1}, \quad (6)$$

where we have used the regulator  $R^\Lambda = (\Lambda^2 - |\mathbf{q}|^2) \Theta(\Lambda^2 - |\mathbf{q}|^2)$ ,  $\Theta$  being the step function.  $\Sigma_b^\Lambda(\Omega, \mathbf{q})$  is the bosonic self-energy. Since the fermionic regulator function has already been set to zero, the fermions naïvely give no contribution to the flow of the bosonic propagator. Hence, following Lee, Strack, and Sachdev, we must define  $\Sigma_b^\Lambda(\Omega, \mathbf{q})$  via the self-consistency relation

$$\Sigma_b^\Lambda(\Omega, \mathbf{q}) = B^\Lambda \frac{|\Omega|}{|\mathbf{q}|}, \quad (7)$$

where  $B^\Lambda$  is the coefficient of the Landau-damping term in the low-frequency expansion,  $|\Omega| \ll v_f^\Lambda |\mathbf{q}|$ , of the particle-hole bubble  $\Pi_{\text{ph}}^\Lambda(\Omega, \mathbf{q}) = (g^\Lambda)^2 \int_{\omega \mathbf{k}} G_f^\Lambda(\omega + \Omega, \mathbf{k} + \mathbf{q}) G_f^\Lambda(\omega, \mathbf{k})$  shown in Fig. 1(b). Since we use a low-frequency expansion, the expression (7) should contain a step function restricting the self-energy to the low-frequency regime. However, including it does not materially change our results, so we omit it for simplicity.

The flow of the Yukawa coupling  $g^\Lambda$  is given by the diagram in Fig. 1(c):

$$\partial_\Lambda g^\Lambda = -(g^\Lambda)^3 \int_{\Omega \mathbf{q}}^R (G_f^\Lambda(\omega + \Omega, \mathbf{k} + \mathbf{q}))^2 D_b^\Lambda(\Omega, \mathbf{q}) \Big|_{\tilde{k}=0, \omega=0}, \quad (8)$$

where we have set external frequencies and momenta to zero ( $\tilde{k} = 0$  for fermions), i.e. we follow only the forward-scattering part of the vertex. The flow equations (5) and (8) and the self-consistency relation (7) completely determine the flow of our truncation of  $\Gamma_R^\Lambda$ .

*Parameterizing the flow.* During the flow, the dependences of the fermionic propagator on the frequency and the momentum (as described by  $A_\omega^\Lambda$  and  $A_k^\Lambda$ ) and the Yukawa coupling ( $g^\Lambda$ ) will all be renormalized. Their dependence on  $\Lambda$  defines a set of anomalous dimensions:  $\eta_\omega^\Lambda$ ,  $\eta_k^\Lambda$ , and  $\eta_g^\Lambda$ . These are given by

$$\eta_\omega^\Lambda = -\frac{d \ln A_\omega^\Lambda}{d \ln \Lambda}; \quad \eta_k^\Lambda = -\frac{d \ln A_k^\Lambda}{d \ln \Lambda}; \quad \eta_g^\Lambda = -\frac{d \ln g^\Lambda}{d \ln \Lambda}. \quad (9)$$

Furthermore it will be useful to introduce the dimensionless variables

$$\tilde{B}^\Lambda = \frac{B^\Lambda}{\Lambda^2}; \quad \tilde{g}^\Lambda = \frac{g^\Lambda}{\sqrt{\Lambda A_\omega^\Lambda A_k^\Lambda}}. \quad (10)$$

The anomalous dimension  $\eta_\omega^\Lambda$  is determined by the scale-dependence of the correction to the  $i\omega$  term in the fermionic self-energy (4). This may be obtained by setting  $\tilde{k}$  to zero on the right-hand side of (5), taking an  $i\omega$ -derivative and the limit  $\omega \rightarrow 0$ :

$$\eta_\omega^\Lambda = 2 (\tilde{g}^\Lambda)^2 \int_{\mathbf{q}}^{|\mathbf{q}| < 1} \int_{\Omega} \frac{1}{(i\Omega - |\mathbf{q}| \cos \theta)^2} \frac{1}{\left(v_f^\Lambda \tilde{B}^\Lambda \frac{|\Omega|}{|\mathbf{q}|} + 1\right)^2}. \quad (11)$$

Note that the integral in (11) depends on the scale only through the combination  $v_f^\Lambda \tilde{B}^\Lambda$ , so (11) defines a function  $f(x)$  by  $\eta_\omega^\Lambda = (\tilde{g}^\Lambda)^2 f(v_f^\Lambda \tilde{B}^\Lambda)$ . The function  $f(x)$  is monotonically increasing with the limiting values  $f(x \rightarrow 0) = 0$  and  $f(x \rightarrow \infty) = 1/\pi^2$ .

Similarly, the anomalous dimension  $\eta_k^\Lambda$  is determined by the scale-dependence of the correction to the  $\tilde{k}$  term in the fermionic self-energy (4). This may be obtained by setting  $\omega$  to zero on the right-hand side of (5) and then taking a  $\tilde{k}$ -derivative:

$$\eta_k^\Lambda = 2 (\tilde{g}^\Lambda)^2 \lim_{\tilde{k} \rightarrow 0} \frac{\partial}{\partial \tilde{k}} \left[ \int_{\mathbf{q}} \int_{\Omega} \frac{1}{(i\Omega - [\tilde{k} + |\mathbf{q}| \cos \theta])} \times \frac{1}{\left(v_f^\Lambda \tilde{B}^\Lambda \frac{|\Omega|}{|\mathbf{q}|} + 1\right)^2} \right]. \quad (12)$$

Again, the part in square brackets depends on the scale only via  $v_f^\Lambda \tilde{B}^\Lambda$ . We note that the  $\tilde{k}$  derivative and the  $\Omega$  integration do not commute; this is a consequence of setting the fermionic regulator function to zero. In terms of the function defined by (11), we find  $\eta_k^\Lambda = (\tilde{g}^\Lambda)^2 [f(v_f^\Lambda \tilde{B}^\Lambda) - f(\infty)]$ .

The particle-hole bubble, Fig. 1(b), determines the bosonic renormalization parameter  $\tilde{B}^\Lambda$ :

$$\tilde{B}^\Lambda = \frac{k_F}{2\pi\Lambda} \frac{(\tilde{g}^\Lambda)^2}{v_f^\Lambda}. \quad (13)$$

Finally, we obtain the anomalous dimension of the Yukawa coupling,  $\eta_g^\Lambda$ , which — because of the structure

of the diagrams shown in Fig. 1 — is precisely equal to minus the fermionic anomalous dimension at all scales,  $\eta_g^\Lambda = -\eta_\omega^\Lambda$ .

*Low-energy fixed point.* From (10), we derive the flow equation:

$$-\Lambda \partial_\Lambda \tilde{g}^\Lambda = \left( \frac{1}{2} + \eta_g^\Lambda - \frac{1}{2} \eta_\omega^\Lambda - \frac{1}{2} \eta_k^\Lambda \right) \tilde{g}^\Lambda. \quad (14)$$

At the start of the flow,  $A_\omega^{\Lambda_{UV}} = A_k^{\Lambda_{UV}} = 1$ . The initial value of  $\tilde{g}^\Lambda$  does not matter, provided that it is non-zero; this is because, in the absence of the bosonic mass term, there are no relevant operators at the fixed point. It is worth noting that, according to (13), a non-zero  $\tilde{g}^{\Lambda_{UV}}$  implies a non-zero  $\tilde{B}^{\Lambda_{UV}}$ ; in other words, we need to include a small amount of Landau damping even in the bare action to get the flow started.

For a finite-coupling fixed point, the term in the brackets on the right-hand side of (14) must be zero, and hence the anomalous dimensions at the fixed point obey  $1 = -2\eta_g + \eta_\omega + \eta_k$ . To determine them, we observe that — according to (13) — if  $\tilde{g}^\Lambda$  remains finite at the fixed point,  $v_f^\Lambda \tilde{B}^\Lambda$  must diverge like  $\Lambda^{-1}$ . This means that we need only compute the limiting values of the right-hand sides of (11) and (12) as  $v_f^\Lambda \tilde{B}^\Lambda \rightarrow \infty$ . The result of these computations is that, at the fixed point,  $\eta_\omega = -\eta_g = (\tilde{g}/\pi)^2$ , while  $\eta_k = 0$ , which implies that

$$\eta_\omega = -\eta_g = \frac{1}{3}; \quad \eta_k = 0; \quad \tilde{g} = \frac{\pi}{\sqrt{3}}. \quad (15)$$

The scaling of the bosonic propagator follows from (13) and (15), whence  $B^\Lambda = \tilde{B}^\Lambda \Lambda^2 \sim \Lambda^{1-\eta_\omega+\eta_k}$ . We interpret  $\Lambda$  as a momentum scale, so that  $B^\Lambda \sim |\mathbf{q}|^{1-\eta_\omega+\eta_k}$ . This yields a Landau-damping term of the form  $|\Omega|/|\mathbf{q}|^{\eta_\omega-\eta_k}$ , whence it follows that  $z_b = 7/3$ :

$$(D_b(\Omega, \mathbf{q}))^{-1} \sim \frac{|\Omega|}{|\mathbf{q}|^{1/3}} + \mathbf{q}^2. \quad (16)$$

The lack of a fermionic regulator in our approach results in an apparent ambiguity when one tries to determine the scaling form of the fermionic Green's function. One option would be to choose a scaling in which the fermionic and bosonic momenta scale together, as in [22]; but in this calculation that appears to be a poor choice for at least two reasons. First, such a choice yields results that do not agree with the one-loop evaluation of the fermionic self-energy [11] when vertex corrections are neglected. Second, if we make that choice then the bosonic and fermionic frequencies scale differently as the fixed point is approached. This suggests that we should rather choose a scaling in which  $\omega \sim \Omega \sim \Lambda^{z_b}$ ; consistency then requires different scaling for the fermionic and bosonic momenta:  $\tilde{k} \sim \Lambda^2$  whereas  $|\mathbf{q}| \sim \Lambda$ . This scaling recovers the one-loop fermionic self-energy when vertex corrections are neglected, and furthermore is precisely the

scaling that is used in patch theories [12, 15–19]. The resulting fermionic propagator has the following  $\tilde{k} = 0$  form at the interacting fixed point:

$$(G_f(\omega, \mathbf{k}_F))^{-1} \sim \omega^{1-(\eta_\omega/z_b)} \sim \omega^{6/7}, \quad (17)$$

and the following form at zero frequency:

$$(G_f(0, \mathbf{k}))^{-1} \sim \tilde{k}^{1-(\eta_k/2)} \sim \tilde{k}. \quad (18)$$

This leads to a fermionic dynamical exponent  $z_f = z_b/2 = 7/6$ . The scaling may also be characterised by a vanishing quasiparticle weight  $Z_f^\Lambda \sim \Lambda^{\eta_\omega} \sim \Lambda^{1/3}$  and a vanishing Fermi velocity  $v_f^\Lambda \sim \Lambda^{\eta_\omega - \eta_k} \sim \Lambda^{1/3}$  as  $\Lambda \rightarrow 0$ . (17) and (18) demonstrate the non-Fermi-liquid character of the fermions at the fixed point. A thermodynamic consequence of this is that, in the non-Fermi-liquid regime above the quantum critical point, the specific heat capacity should depend on temperature as  $C(T) \sim T^{1/z_f} \sim T^{6/7}$  [26]. Note that there is no renormalization of the exponent of  $\tilde{k}$  in (18). It is known [11] that the one-loop fermionic self-energy calculated using a Landau-damped bosonic propagator and a Fermi-liquid fermionic propagator goes as  $\tilde{k}$ , in the light of which this result might have been expected.

In summary, the fermionic and bosonic dynamical exponents are given respectively by

$$z_b = \frac{7}{3}; \quad z_f = \frac{z_b}{2} = \frac{7}{6}. \quad (19)$$

Equations (16–19) constitute the main results of this Letter.

*Discussion.* To compare our results with the literature on this problem, we must extend them to the case in which the fermions come in a large number of flavors,  $N_f$ . This extension is straightforward:  $N_f$  appears only in those diagrams containing a fermion loop, so the only place in which it enters is in the determination of  $v_f^\Lambda \tilde{B}^\Lambda$ . Since this is in any case infinite at the fixed point, altering the value of  $N_f$  makes no difference to our results.

As mentioned above, the  $z_f = z_b/2$  scaling that we have chosen matches that used in patch theories. However, to be forced to this scaling at the fixed point is not the same as assuming it from the beginning; our calculation begins with a full Fermi surface, not a set of patches. As a result we see low-energy behavior that is inconsistent with that obtained using a patch approach. In particular, the Landau damping of our bosonic propagator is unambiguously renormalized for any  $N_f$ , unlike in a patch theory where one finds no corrections to the conventional  $|\Omega|/|\mathbf{q}|$  form. This is due to the importance, in our calculation, of the vertex correction (Fig. 1(c)):  $\eta_g = -\eta_\omega$  at all stages in the flow, including at the fixed point.

For comparison with experiments, it would be helpful to know how robust the numerical values of our exponents are to extensions of the truncation scheme used

for  $\Gamma_R^\Lambda$ . The most obvious term to include would be the bosonic mass: in our calculation this was set to zero throughout, but it should more properly be tracked during the flow. If we wish to include the possibility of superconductivity in the vicinity of the quantum critical point, analysing the effect of four-fermion interactions is also important. Lastly, there is the question of whether the multi-boson interaction vertices, neglected in this treatment, remain well behaved at the fixed point. Even if they do, we would expect them to alter the anomalous dimensions, and in particular to give a non-zero  $\eta_k$  [16, 17, 22].

A clear experimental prediction of our work is that the Landau-damping rate  $\Gamma_{\mathbf{q}} \sim |\mathbf{q}|^{1/3}$ , rather than the usually expected  $\Gamma_{\mathbf{q}} \sim |\mathbf{q}|$ . This calls to mind the measurements taken some years ago on UGe<sub>2</sub> [27] and more recently on other similar compounds [28], which appear to show a damping rate that does not extrapolate to zero in the  $|\mathbf{q}| \rightarrow 0$  limit. At least two theories have been proposed [29, 30] in which it would not be expected to. However, our work suggests that the extrapolation should be done with a damping rate  $\Gamma_{\mathbf{q}} \sim |\mathbf{q}|^\alpha$  (with  $0 < \alpha < 1$ ) rather than the conventional one. There are good reasons for writing a general  $\alpha$  here. First, our analysis above is for the strict  $d = 2$  limit; UGe<sub>2</sub>, while exhibiting some anisotropy in its resistivity [31], is certainly a three-dimensional crystal. Second, it seems likely that improvements to our truncation scheme would change the theoretically predicted exponent even in the  $d = 2$  case.

Finally, we discuss some of the implications of our work for the antiferromagnetic critical point. Our analysis above sheds some light on an unresolved issue in the paper by Lee, Strack, and Sachdev, viz. why  $z_b = z_f$ . The fact that the scaling of the bosonic self-energy is fully determined by the low-frequency expansion of the particle-hole bubble enforces  $z_b = z_f$  at the antiferromagnetic fixed point. This is a trivial variation of our argument above that  $z_b = 2z_f$  in the ferromagnetic case. In the antiferromagnetic case, the fixed point presented in [21] is for  $N_f = 1$  while the diagrammatics are valid for  $N_f \gg 1$ , so we cannot directly assess whether they agree or not. The extension of the antiferromagnetic fRG analysis to the  $N_f \gg 1$  case will result in changes to the anomalous dimensions at the fixed point; carrying out this work would provide a useful benchmark of fRG against other methods.

*Acknowledgments.* We thank A.V. Chubukov and A.M. Tsvelik for useful discussions, and A.D. Huxley for drawing the case of UGe<sub>2</sub> to our attention. Financial support from the EPSRC (UK) under grants EP/G03673X/1 (SPR) and EP/I031014/1 (CAH) is gratefully acknowledged.

- 
- [1] P. A. Lee, N. Nagaosa, and X.-G. Wen, *Rev. Mod. Phys.* **78**, 17 (2006).
- [2] G. R. Stewart, *Rev. Mod. Phys.* **73**, 797 (2001).
- [3] H. von Löhneysen, A. Rosch, M. Vojta, and P. Wölfle, *Rev. Mod. Phys.* **79**, 1015 (2007).
- [4] C. Pfleiderer, D. Reznik, L. Pintschovius, H. von Löhneysen, M. Garst, and A. Rosch, *Nature* **427**, 227 (2004).
- [5] J. A. Hertz, *Phys. Rev. B* **14**, 1165 (1976).
- [6] A. J. Millis, *Phys. Rev. B* **48**, 7183 (1993).
- [7] S. Thier and W. Metzner, *Phys. Rev. B* **84**, 155133 (2011).
- [8] A. L. Fitzpatrick, S. Kachru, J. Kaplan, and S. Raghu, *Phys. Rev. B* **88**, 125116 (2013).
- [9] A. L. Fitzpatrick, S. Kachru, J. Kaplan, and S. Raghu, *Phys. Rev. B* **89**, 165114 (2014).
- [10] T. Holstein, R. E. Norton, and P. Pincus, *Phys. Rev. B* **8**, 2649 (1973).
- [11] M. Reizer, *Phys. Rev. B* **40**, 11571 (1989).
- [12] J. Polchinski, *Nuc. Phys. B* **422**, 617 (1994).
- [13] B. L. Altshuler, L. B. Ioffe, and A. J. Millis, *Phys. Rev. B* **50**, 14048 (1994).
- [14] J. Rech, C. Pépin, and A. V. Chubukov, *Phys. Rev. B* **74**, 195126 (2006).
- [15] S.-S. Lee, *Phys. Rev. B* **80**, 165102 (2009).
- [16] M. A. Metlitski and S. Sachdev, *Phys. Rev. B* **82**, 075127 (2010).
- [17] D. F. Mross, J. McGreevy, H. Liu, and T. Senthil, *Phys. Rev. B* **82**, 045121 (2010).
- [18] D. Dalidovich and S.-S. Lee, *Phys. Rev. B* **88**, 245106 (2013).
- [19] S. Sur and S.-S. Lee, *Phys. Rev. B* **90**, 045121 (2014).
- [20] G. Torroba and H. Wang, arXiv:1406.3029.
- [21] J. Lee, P. Strack, and S. Sachdev, *Phys. Rev. B* **87**, 045104 (2013).
- [22] C. Drukier, L. Bartosch, A. Isidori, and P. Kopietz, *Phys. Rev. B* **85**, 245120 (2012).
- [23] C. Wetterich, *Phys. Lett. B* **301**, 90 (1993).
- [24] T. R. Morris, *Int. J. Mod. Phys. A* **9**, 2411 (1994).
- [25] W. Metzner, M. Salmhofer, C. Honerkamp, V. Meden, and K. Schönhammer, *Rev. Mod. Phys.* **84**, 299 (2012).
- [26] T. Senthil, *Phys. Rev. B* **78**, 035103 (2008).
- [27] A. D. Huxley, S. Raymond, and E. Ressouche, *Phys. Rev. Lett.* **91**, 207201 (2003).
- [28] C. Stock, D. Sokolov, P. Bourges, P. Tobash, K. Gofryk, F. Ronning, E. Bauer, K. Rule, and A. Huxley, *Phys. Rev. Lett.* **107**, 187202 (2011).
- [29] V. P. Mineev, *Phys. Rev. B* **88**, 224408 (2013).
- [30] A. V. Chubukov, J. J. Betouras, and D. V. Efremov, *Phys. Rev. Lett.* **112**, 037202 (2014).
- [31] Y. Onuki, I. Ukon, S. Yun, I. Umehara, K. Satoh, T. Fukuhara, H. Sato, S. Takayanagi, M. Shikama, and A. Ochiai, *J. Phys. Soc. Japan* **61**, 293 (1992).